J|A|C|S ARTICLES

Published on Web 04/22/2010

Evidence of Dynamic Pentagon−Heptagon Pairs in Single-Wall Carbon Nanotubes using Surface-Enhanced Raman Scattering

Toshihiko Fujimori,[†] Koki Urita,[‡] Tomonori Ohba,[†] Hirofumi Kanoh,[†] and Katsumi Kaneko*,[†]

Department of Chemistry, Graduate School of Science, Chiba University, 1-33 Yayoi, Inage, Chiba 263-8522, Japan, and Department of Applied Chemistry, Faculty of Engineering, Nagasaki University, 1-14 Bunkyo-machi, Nagasaki-shi, Nagasaki 852-8521, Japan

Received January 28, 2010; E-mail: kaneko@pchem2.s.chiba-u.ac.jp

Abstract: Surface-enhanced Raman scattering (SERS) was applied to detecting pentagon−heptagon pairs, the so-called Stone−Wales defect, in single-wall carbon nanotubes (SWCNTs). When a probing laser light was scanned over a SWCNT-dispersed silver surface, two distinct SERS spectra were obtained: (1) temporally stable spectra similar to that of resonance Raman spectra of bulk SWCNTs and (2) temporally fluctuating spectra with additional peaks which were not observed in the non-SERS spectra. The fluctuations in the SERS spectra are discussed in association with dynamic reconstruction of defective structures of SWCNTs (nonhexagonal arrangements of carbon atoms) in the vicinity of SERS-active sites under irradiation of the laser light.

Introduction

All carbon atoms comprising a single-wall carbon nanotube (SWCNT) are regarded as surface atoms. This feature offers the possibility of SWCNTs as a candidate for materials providing superhigh surface areas.[1,2] For wide application of the material, in addition to a high surface area, elucidation of its surface chemistry is essential. Surface defects play a critical role in surface chemistry; for example, molecules react with topological defects to vary the surface property and catalyst metal atoms can be favorably adsorbed on so-called topological defects in the graphene wall.[3] Defects in SWCNTs should be essential in various chemical and physical properties of SWCNTs.[4−6] It is thus necessary to investigate the defect-associated nature of SWCNTs for their use in chemical and physical applications.[7]

Raman spectroscopy is widely applied to carbon materials as a characterization tool for defects. Every possible defect is thought to induce a so-called D band.[8] The plausible assignment of the D band is ascribed to a phonon mode that stems from the hexagonal structure of graphite.[8,9] The hexagon, however, is not the only possible configuration for atoms in a carbon nanotube; that is, pentagon, heptagon, and octagon configurations, referred to as topological defects,[10−13] are also possible candidates for geometrical units in carbon nanotubes. Suenaga et al. succeeded in observing topological defects on an SWCNT using a sophisticated high-resolution transmission electron microscopy (TEM) technique.[14] The presence of topological defects changes the symmetry of a carbon nanotube, such that characteristic vibrational modes associated with the topological defects are expected. Such vibrational modes have not been experimentally confirmed by Raman spectroscopy for nanotubes thus far. However, a vibrational mode localized on a closed-cap structure of a SWCNT, for example, was investigated by inelastic electron tunneling spectroscopy.[15]

An ultrasensitive technique is thus required for probing vibrational modes associated with topological defects. Surface-enhanced Raman scattering (SERS)[16−21] satisfies this require-

[†] Chiba University.
[‡] Nagasaki University.

(1) Kaneko, K.; Ishii, C.; Ruike, M.; Kuwabara, H. *Carbon* **1992**, *30*, 1075.
(2) Peigney, A.; Laurent, Ch.; Flahaut, E.; Bacsa, R. R.; Rousset, A. *Carbon* **2001**, *39*, 507.
(3) Meng, F. Y.; Zhou, L. G.; Shi, S.-Q.; Yang, R. *Carbon* **2003**, *41*, 2023.
(4) Bettinger, H. F. *J. Phys. Chem. B* **2005**, *109*, 6922.
(5) Nardelli, M. B.; Yakobson, B. I.; Bernholc, J. *Phys. Rev. Lett.* **1998**, *81*, 4656.
(6) Choi, H. J.; Ihm, J.; Louie, S. G.; Cohen, M. L. *Phys. Rev. Lett.* **2000**, *84*, 2917.
(7) Charlier, J.-C. *Acc. Chem. Res.* **2002**, *35*, 1063.
(8) Tuinstra, F.; Koenig, J. L. *J. Chem. Phys.* **1970**, *53*, 1126.
(9) Saito, R.; Jorio, A.; Filho, A. G. S.; Grueners, A.; Pimenta, M. A.; Dresselhaus, G.; Dresselhaus, M. S. *Physica B* **2002**, *323*, 100.
(10) Mackay, A. L.; Terrones, H. *Nature* **1991**, *352*, 762.
(11) Lenosky, T.; Gonze, X.; Teter, M.; Elser, V. *Nature* **1992**, *355*, 333.
(12) Saito, R.; Dresselhaus, G.; Dresselhaus, M. S. *Chem. Phys. Lett.* **1992**, *195*, 537.
(13) Iijima, S.; Ichihashi, T.; Ando, Y. *Nature* **1992**, *356*, 776.
(14) Suenaga, K.; Wakabayashi, H.; Koshino, M.; Sato, Y.; Urita, K.; Iijima, S. *Nat. Nanotech.* **2007**, *2*, 358.
(15) Vitali, L.; Burghard, M.; Schneider, M. A.; Liu, L.; Wu, S. Y.; Jayanthi, C. S.; Kern, K. *Phys. Rev. Lett.* **2004**, *93*, 136103.
(16) Nie, S.; Emory, S. R. *Science* **1997**, *275*, 1102.
(17) Kneipp, K.; Kneipp, H.; Itzkan, I.; Dasari, R. R.; Feld, M. S. *Chem. Rev.* **1999**, *99*, 2957.
(18) Kneipp, K.; Wang, Y.; Kneipp, H.; Perelman, L. T.; Itzkan, I.; Dasari, R. R.; Feld, M. S. *Phys. Rev. Lett.* **1997**, *78*, 1667.
(19) Otto, A. *J. Raman Spectrosc.* **2002**, *33*, 593.
(20) Weiss, A.; Haran, G. *J. Phys. Chem. B* **2001**, *105*, 12348.
(21) Bizzarri, A. R.; Cannistraro, S. *Phys. Rev. Lett.* **2005**, *94*, 068303.

10.1021/ja100760m

ment, due to the huge enhancement of the Raman cross-section in the vicinity of metal surfaces (for example, assemblies of nanoparticles or rough surfaces of noble metals) in SERS.[22] The SERS phenomenon stems mainly from two mechanisms: surface plasmon resonance and/or resonance accompanying the electronic transition between a metal and a molecule.[22] Under contribution from an extremely small number of molecules, ensemble averaging turns out to be the specific behavior from each molecule. This may give rise to temporal fluctuations of intensities and frequencies.[21] An intriguing phenomenon is the migration of topological defects on an SWCNT surface under electron irradiation.[14]

In this context, we attempted to detect the dynamic behavior of topological defects on SWCNTs using Raman spectroscopy, which can be widely applied to SWCNTs in environments of various gases and liquids. In this letter, we report temporally fluctuating SERS spectra from SWCNTs, which can be assigned to the dynamic behavior of topological defects.

Experimental Section

Purified SWCNTs produced by a laser ablation method were used.[23,24] A silver foil (purity 99.95%, 0.015 mm thickness) was purchased from Wako Pure Chemical Industries, Ltd., and used as the SERS-active metal. The surface geometry of the silver foil was examined by scanning electron microscopy (SEM) and was found to have partially a step and terrace structure with an interval of ∼100 nm (see the Supporting Information, Figure S1). The SWCNT sample was added to trichloroethylene and sonicated for 30 min. A droplet of the SWCNT-dispersed trichloroethylene solution was dropped onto the silver foil, which was washed by ethanol with sonication before adding the solution. The SWCNT-dispersed silver foil was then pretreated in an in situ Raman cell (Japan High Tech Co. Ltd., Model MVH-5) at 423 K under 2×10^{-3} Pa pressure for 2 h. After natural cooling to ambient temperature without exposure to air, SERS measurements were carried out with a single-monochromator micro-Raman spectrometer using a backscattering configuration (JASCO NRS-3100) under vacuum. For the in situ Raman cell, a 20× long-distance objective was used. SERS measurements were conducted with 532 nm (Nd:YAG laser) and 632.8 nm (He−Ne laser) excitation. The laser power density was $\sim 10^8$ W m^{-2} at the sampling points. A collection time of 10 s was used for each SERS measurement.

Results and Discussion

When the probing laser light ($\lambda = 532$ nm) was scanned over the silver surface dispersing SWCNTs, two types of SERS spectra were obtained: (1) one similar to a non-SERS spectrum without any temporal fluctuation of frequencies and intensities (Figure 1) and (2) SERS spectra exhibiting additional peaks, absent in a non-SERS spectrum (Figure 2). The latter case shows strong spectral fluctuation with time. The time interval was ∼10 s between the acquisition of two spectra.

For the SERS spectrum (1) shown in Figure 1, a narrower peak of the so-called G^+ band centered at ∼1590 cm^{-1} compared to the bulk spectrum is seen. A normalized non-SERS spectrum of the bulk sample is also shown in Figure 1 for clarity. The minimum value of the full width at half-maximum (fwhm) of the G^+ band in the SERS spectrum obtained by our measurements is 9.6 cm^{-1}. This value is very close to that of the natural fwhm of an ideal SWCNT (∼10 cm^{-1}),[25] indicating that the SERS spectrum is the consequence of a small number of SWCNTs or even down to single SWCNT detection. It was also confirmed for single SWCNT detection that the frequency of the G^+ band is not averaged out in the SERS spectra and deviates from position to position due to the varying chirality of SWCNTs[26] (see the Supporting Information, Figure S2). The SERS spectrum (1) is in good agreement with previously reported results.[25,27]

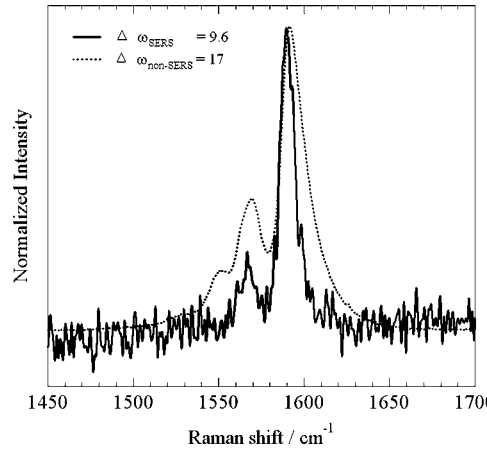

Figure 1. Selected SERS spectrum (1) and a non-SERS spectrum from the bulk sample, indicated by solid line and dotted lines, respectively. The fwhm of the G^+ band at ∼1590 cm^{-1} is given by $\Delta\omega$ (cm^{-1}). Both spectra were recorded with 532 nm excitation. The narrowing of the G^+ band on the SERS spectrum implies a small number of SWCNTs, even single SWCNT detection.

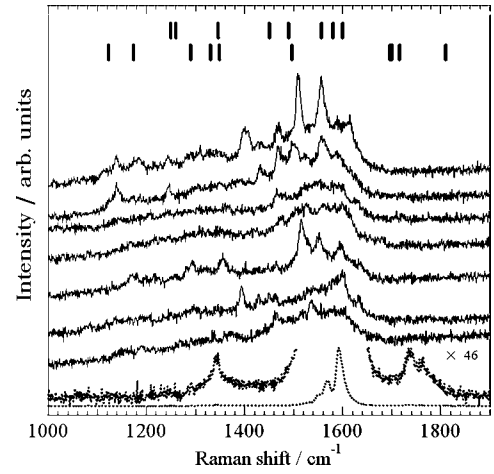

Figure 2. Temporally fluctuating SERS spectra (2) (solid lines) and a non-SERS spectrum (dotted line) from the bulk sample. A magnified (46×) Raman spectrum for the non-SERS spectrum is also shown for clarifying the obtained weak Raman signals. Each SERS spectrum was acquired from the bottom to the top with a time interval of ∼10 s. The upper and lower bars at the top indicate calculated frequencies for graphite, which are predicted by the double-resonance theory,[9] and graphene with an STW defect (scaled by a factor of 0.9943 from the frequencies reported in reference[48]), respectively. Each spectrum was recorded with 532 nm excitation.

(22) Campion, A.; Kambhampati, P. *Chem. Soc. Rev.* **1998**, *27*, 241.
(23) Yudasaka, M.; Kokai, F.; Takahashi, K.; Yamada, R.; Sensui, N.; Ichihashi, T.; Iijima, S. *J. Phys. Chem. B* **1999**, *163*, 3576.
(24) Kokai, F.; Takahashi, K.; Yudasaka, M.; Iijima, S. *J. Phys. Chem. B* **2000**, *104*, 6777.
(25) Kneipp, K.; Kneipp, H.; Corio, P.; Brown, S. D. M.; Shafer, K.; Motz, J.; Perelman, L. T.; Hanlon, E. B.; Marucci, A.; Dresselhaus, G.; Dresselhaus, M. S. *Phys. Rev. Lett.* **2000**, *84*, 3470.
(26) Jorio, A.; Pimenta, M. A.; Filho, A. G. S.; Saito, R.; Dresselhaus, G.; Dresselhaus, M. S. *New J. Phys.* **2003**, *5*, 139.
(27) Teredesai, P. V.; Sood, A. K.; Govindaraj, A.; Rao, C. N. R. *Appl. Surf. Sci.* **2001**, *182*, 196.

An intriguing case is the SERS spectra (2) in Figure 2, which show much richer spectral information than the SERS spectrum (1) shown in Figure 1. A number of unexpected peaks are obvious in the SERS spectra shown in Figure 2. Furthermore, these peaks exhibit intense temporal fluctuations. In general, temporal fluctuations of peak frequencies and intensities are often observed in SERS measurements.[16,18,20,21,28−35] This phenomenon is usually referred to as the blinking effect. Though interpretations of this blinking effect are still controversial and are under discussion, surface diffusion of molecules[16,20,21] against so-called "hot spots" on SERS-active metals, where strong enhancement may occur, and photoinduced structural changes[28,35] are possible explanations of the blinking effect. Since an SWCNT is too large to diffuse on the silver surface under our experimental conditions, the fluctuations could be attributed to structural changes in the SWCNT in the vicinity of SERS-active sites. High-resolution TEM investigations have revealed that topological defects migrate on the hexagonal surface under electron irradiation.[14,36−39] We infer from experimental results by TEM observations that tentative assignment of the fluctuating SERS peaks turn to vibration modes related to topological defects.

We first discuss assignments for SERS peaks, which are absent in the non-SERS spectrum, considering the ideal structures of SWCNTs. Group theory predicts 15 or 16 Raman-active modes and 6−9 infrared (IR) -active modes for an ideal SWCNT, depending on the chirality.[40] An IR-active mode may not be ruled out for SERS spectra, because matter is influenced by a strong electric field.[41] On the basis of the relation between band gap energies and diameter of the SWCNT, the so-called Kataura plot,[42] the SWCNT sample used in this study is dominantly in resonance with semiconducting SWCNTs under 532 nm excitation (see the Supporting Information, Figure S3(a)). This indicates that predicted Raman-[43−45] or IR-active[43,46] modes of armchair SWCNTs can be tentatively ruled out, since armchair SWCNTs are classified as metallic SWCNTs. Though the presence of metallic SWCNTs in the SWCNT sample is confirmed by the 632.8 nm excitation (see the Supporting Information, Figure S3(b)), semiconducting SWCNTs are selectively probed under 532 nm excitation due to enhancements in combination with SERS and resonance Raman scattering, which occurs when an excitation light accompanies the electronic transition of an SWCNT. SERS spectra of an SWCNT sample recorded using 632.8 nm excitation are shown in the Supporting Information, Figure S4. Since the SWCNT sample also includes carbon impurities (for example, amorphous carbon and graphite), vibrational modes for graphite should be taken into account. The double-resonance theory can explain experimentally observed weak Raman signals of graphite, which are not well understood.[9] The calculated frequencies of graphite with an excitation energy of 2.33 eV ($\lambda = 532$ nm) are shown in Figure 2 as bars (top of the plot). Some of the theoretical values seem to be related to the SERS signals; the obtained SERS spectra, however, show more peaks than the calculated spectrum. We focus on the SERS signals observed around 1100−1200 cm^{-1} because theoretically obtained first-order frequencies both for the semiconducting SWCNTs[43,45,46] and graphite[9] are absent in this frequency region.

Assignments for the observed SERS peaks depend on theoretical calculations of Raman spectra using the second-generation reactive empirical bond order (REBO) potential[47] for graphene with a specific arrangement of pentagon−heptagon pairs known as a Stone−Wales defect (SW defect).[48] Though the term SW defect is widely used,[49] we will use a new term, Stone−*Thrower*−Wales defect (STW defect), instead of SW defect hereafter.[50] According to an expression by Wu and Dong,[48] some of the calculated peaks could be ascribed to atomic motions localized on an STW defect. The frequency values of the localized modes are shown in Figure 2 as bars (lower set). Since the calculated frequency for perfect graphene slightly overestimates the G band frequency (1591 cm^{-1}),[48] the frequencies for graphene with an STW defect are scaled by a factor of 0.9943 (=1582 cm^{-1}/1591 cm^{-1}). Here, the G band frequency at 1582 cm^{-1} was used as the standard value.[43]

Figure 3 shows a selected SERS spectrum, with explicit peaks around 1100−1200 cm^{-1}. The inset in Figure 3 shows a magnified spectrum with Lorentzian fits around 1100−1200 cm^{-1}. Since the vibrational modes related to perfect SWCNTs and graphite can be ruled out around 1100−1200 cm^{-1}, we assign the observed peaks at 1139 and 1183 cm^{-1} to those predicted at 1122 and 1173 cm^{-1} for STW defects, respectively. These peaks are also dominant in the SERS spectra of single-wall carbon nanohorns,[51] composed of an aggregation of defective tubular structures of a graphene layer. In particular, for the theoretical vibrational mode at 1173 cm^{-1}, a correspond-

(28) Perevedentseva, E.; Karmenyan, A.; Chung, P.-H.; Cheng, C.-L. *J. Vac. Sci. Technol. B* **2005**, *23*, 1980.
(29) Moyer, P. J.; Schmidt, J.; Eng, L. M.; Meixner, A. J. *J. Am. Chem. Soc.* **2000**, *122*, 5409.
(30) Kudelski, A. *J. Raman Spectrosc.* **2007**, *38*, 1494.
(31) Kudelski, A. *Chem. Phys. Lett.* **2006**, *427*, 206.
(32) Veres, M.; Füle, M.; Tóth, S.; Koós, M.; Pócsik, I. *Diamond Relat. Mater.* **2004**, *13*, 1412.
(33) Andersen, P. C.; Jacobson, M. L.; Rowlen, K. L. *J. Phys. Chem. B* **2004**, *108*, 2148.
(34) Suh, J. S.; Moskovits, M.; Shakhesemampour, J. *J. Phys. Chem.* **1993**, *97*, 1678.
(35) Bjerneld, E. J.; Svedberg, F.; Johansson, P.; Käll, M. *J. Phys. Chem. A* **2004**, *108*, 4187.
(36) Meyer, J. C.; Kisielowski, C.; Erni, R.; Rossell, M. D.; Crommie, M. F.; Zettl, A. *Nano Lett.* **2008**, *8*, 3582.
(37) Hashimoto, A.; Suenaga, K.; Gloter, A.; Urita, K.; Iijima, S. *Nature* **2004**, *430*, 870.
(38) Huang, J. Y.; Chen, S.; Ren, Z. F.; Wang, Z. Q.; Wang, D. Z.; Vaziri, M.; Suo, Z.; Chen, G.; Dresselhaus, M. S. *Phys. Rev. Lett.* **2006**, *97*, 075501.
(39) Yoon, M.; Han, S.; Kim, G.; Cee, S. B.; Berber, S.; Osawa, E.; Ihm, J.; Terrones, M.; Banhart, F.; Charlier, J.-C.; Grobert, N.; Terrones, H.; Ajayan, P. M.; Tománek, D. *Phys. Rev. Lett.* **2004**, *92*, 075504.
(40) Saito, R.; Dresselhaus, G.; Dresselhaus, M. S. *Physical Properties of Carbon Nanotubes*; Imperial College Press: London, 1998.
(41) Ayars, E. J.; Hallen, H. D.; Jahncke, C. L. *Phys. Rev. Lett.* **2000**, *85*, 4180.
(42) Kataura, H.; Kumazawa, Y.; Maniwa, Y.; Umezu, I.; Suzuki, S.; Ohtsuka, Y.; Achiba, Y. *Synth. Met.* **1999**, *103*, 2555.
(43) Eklund, P. C.; Holden, J. M.; Jishi, R. A. *Carbon* **1995**, *33*, 959.
(44) Rao, A. M.; Richter, E.; Bandow, S.; Chase, B.; Eklund, P. C.; Williams, K. A.; Fang, S.; Subbaswamy, K. R.; Menon, M.; Thess, A.; Smalley, R. E.; Dresselhaus, G.; Dresselhaus, M. S. *Science* **1997**, *275*, 187.
(45) Saito, R.; Takeya, T.; Kimura, T.; Dresselhaus, G.; Dresselhaus, M. S. *Phys. Rev. B* **1998**, *57*, 4145.
(46) Kim, U. J.; Liu, X. M.; Furtado, C. A.; Chen, G.; Saito, R.; Jiang, J.; Dresselhaus, M. S.; Eklund, P. C. *Phys. Rev. Lett.* **2005**, *95*, 157402.
(47) Brenner, D. W.; Shenderova, O. A.; Harrison, J. A.; Stuart, S. J.; Ni, B.; Sinnott, S. B. *J. Phys.: Condens. Matter* **2002**, *14*, 783.
(48) Wu, G.; Dong, J. *Phys. Rev. B* **2006**, *73*, 245414.
(49) Stone, A. J.; Wales, D. J. *Chem. Phys. Lett.* **1986**, *128*, 501.
(50) P. Thrower indicated formation of a pentagon−heptagon pair on radiation-damaged graphite in 1969: Walker, P. L., Jr., Ed. *The Study of Defects in Graphite by Transmission Electron Microscopy, Chemistry and Physics of Carbon*; Marcel Dekker: New York, 1962; Vol. 5, p 262.
(51) Fujimori, T.; Urita, K.; Aoki, Y.; Kanoh, H.; Ohba, T.; Yudasaka, M.; Iijima, S.; Kaneko, K. *J. Phys. Chem. C* **2008**, *112*, 7552.

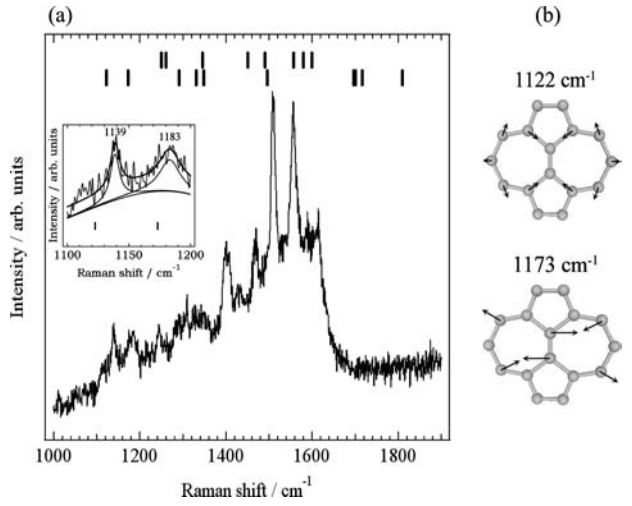

Figure 3. (a) Selected SERS spectrum exhibiting explicit peaks around 1100−1200 cm^{-1} recorded with 532 nm excitation. The bars indicate calculated vibrational modes, the same as in Figure 2. The inset shows a magnified SERS spectrum around 1100−1200 cm^{-1}. A fitting line with two components of the Lorentzian function is indicated by the bold line in the inset. The characteristic vibrational frequencies related to the STW defect around 1100−1200 cm^{-1} are shown by bars. Experimental values around this frequency region are 1139 and 1183 cm^{-1}. (b) Selected vibrational modes associated with the STW defect.[48] The dominant atomic motions are excluded in ref 48.

ing local vibrational state is also predicted by Vandescuren et al. for (10,10) SWCNT,[52] the diameter of which is close to that of the SWCNT sample used in this study. According to their calculation,[52] the vibrational mode shows a slight decrease when the tube diameter increases, converging to that of graphene (a frequency shift of 9 cm^{-1} from the frequency for (10,10) SWCNT). When the frequency shift due to the curvature of a graphene layer is taken into account, the vibrational mode at 1173 cm^{-1} shows a value closer to the experimental value at 1183 cm^{-1}. Both the SERS peaks, at 1139 and 1183 cm^{-1}, show intense fluctuations with time, likely indicating diffusion of pentagonal and heptagonal arrangements consisting of STW defects and/or reconstruction of STW defects. It is ambiguous whether an STW defect is inherently present in the SWCNT or is induced by an enhanced electric field in the vicinity of a SERS-active site; however, as can be seen in the polymerization of C_{60},[53] C−C bond reconstructions could be induced by a laser power density of $\sim 10^8$ W m^{-2} (see the Supporting Information, Figure S5). Since the SWCNTs are exposed to extremely high temperatures during the growth process by laser ablation, topological defects including STW defects should be built into the SWCNT surface during the synthesis process.[54] The above results strongly suggest the potential of the SERS technique to further develop SWCNT-related science and technology. Since SERS can probe type (1) and (2) SERS spectra which are assigned to a highly crystalline and a defective SWCNT, respectively, the SERS technique can be applied to probe the crystallinity evaluation of a single SWCNT.

Another characteristic vibrational mode localized on an STW defect is predicted at 1810 cm^{-1}. This mode is fully localized on a C−C bond centered at a STW defect, and its vibrational frequency depends on orientation of the C−C bond with respect to the tube axis.[55] According to the calculation for (3,3) SWCNT with an STW defect by Miyamoto et al.,[55] tilting of the C−C bond from an orientation parallel to the tube axis causes a frequency shift from 1962 to 1450 cm^{-1} due to the curvature of the SWCNT. A missing SERS peak around 1810 cm^{-1} implies that the C−C bond centered at the STW defect may be tilted with respect to the observed tube axis.

Conclusions

In conclusion, temporal fluctuations of the SERS spectra of an SWCNT are ascribed to dynamic behavior of an STW defect in the SWCNT. Theoretical frequencies at 1122 and 1173 cm^{-1} for the STW defect are evidenced by the SERS method. The higher frequency mode predicted at 1810 cm^{-1} is missing in our experimental observations, probably due to the effect of orientation of the C−C bond centered at an STW defect. Since two types of SERS spectra are observed, that is, (1) a pattern similar to that of the non-SERS spectrum except for the fwhm narrowing and (2) a strongly fluctuating spectral feature offering dynamic behavior of an STW defect, the SERS spectra (1) and (2) indicate probing of highly crystalline and defective regions of the SWCNT, respectively, which allows for characterizing crystallinity in a single SWCNT. This indicates that the SERS technique can be applied to evaluation of the local crystallinity of SWCNTs.

Acknowledgment. We thank Dr. K. Takahashi at the Institute of Research and Innovation (IRI) for providing the SWCNT samples. T.F. thanks Dr. M. Vandescuren and Professor R. Saito for their fruitful comments.

Supporting Information Available: Figures giving an SEM image of the SERS-active silver foil, SERS spectra obtained at probing positions different from those shown in the main article, experimental evidence that semiconducting SWCNTs are in resonance with 532 nm excitation for the SWCNT sample, SERS spectra of the SWCNT recorded with 632.8 nm excitation, and photoinduced polymerization of C_{60} under SERS measurement. This material is available free of charge via the Internet at http://pubs.acs.org.

JA100760M

(52) Vandescuren, M.; Amara, H.; Langlet, R.; Lambin, Ph. *Carbon* **2007**, *45*, 349.
(53) Rao, A. M.; Zhou, P.; Wang, K.-A.; Hager, G. T.; Holden, J. M.; Wang, Y.; Lee, W.-T.; Bi, X.-X.; Eklund, P. C.; Cornett, D. S.; Duncan, M. A.; Amster, I. J. *Science* **1993**, *259*, 955.
(54) Charlier, J.-C.; Terrones, M.; Banhart, F.; Grobert, N.; Terrones, H.; Ajayan, P. M. *IEEE Trans. Nanotechnol.* **2003**, *2*, 349.
(55) Miyamoto, Y.; Rubio, A.; Berber, S.; Yoon, M.; Tomanek, D. *Phys. Rev. B* **2004**, *69*, 121413 R.